SMALL-SIGNAL FREQUENCY RESPONSE THEORY FOR PIECEWISE-CONSTANT TWO-SWITCHED-NETWORK DC-TO-DC CONVERTER SYSTEMS

BILLY Y. LAU and R. D. MIDDLEBROOK

Power Electronics Group
California Institute of Technology

ABSTRACT

Small-Signal Frequency Response Theory is a theory for calculating the output spectrum of ideal dc-to-dc converter systems, i.e. systems with system coefficients piecewise constant in time, for a given spectrum of the signal injected into the control-input, in the small-signal limit. This theory, unlike other methods, can be applied to both resonant and PWM converters, and gives analytic results in closed form for ideal converters. This paper discusses the special case of ideal two-switched-network converter systems in PWM, programmed, and bang-bang operation. For the examples under study, theoretical prediction and experimental results are found to differ by at most 2dB in amplitude and 10 degrees in phase at most frequencies up to three times the switching frequency. Examples are given in this paper for which the theory gives the correct prediction, while other methods fail.

In designing a system, one of the most important objectives is to achieve high performance. The commonly used and relatively inexpensive way to improve system performance is to apply feedback to the system. In designing high-performance dc-to-dc converter systems, feedback is also used to improve system performance. There are many methods that can be used to design and implement feedback-controlled dc-to-dc converter systems, of which linear analog control is probably the most widely used method. This method is effective and economical even though it may not always be the best available method. The digital control method is good in principle but impractical for dc-to-dc converter systems switching at high frequency (higher than 20kHz) because of the computation power required. Moreover, there are technical difficulties in sampling all the states of converter systems at the switching frequency.

In order to design a controller for a plant, a necessary piece of information is the response of the plant, in the frequency domain and/or the time domain, to a set of excitations at its control-inputs. When the plant is a dc-to-dc converter, this information is its response to excitation at its control-inputs in the frequency domain. In most cases, the frequency response is more convenient and more useful for controller design and measurement. In fact, it is next to impossible to measure the small-signal time domain response of a dc-to-dc converter system accurately. Therefore, calculating the control-input to output frequency domain response of a dc-to-dc converter system is essential in order to design a controller.

Much effort has been devoted to finding methods for calculating the frequency domain response of dc-to-dc converter systems. These methods follow three major schools of thought. Representative works which demonstrate these three schools of thought are: *State Space Averaging Modelling Method* by Middlebrook and Ćuk[1], *Sampled-Data Modelling of Switching Converters* by Brown[2], and *Small-Signal Analysis of Resonant Converters* by Vorpérian[3]. All these methods are based on the idea of *"averaging"*. They work only with ideal dc-to-dc converter systems, i.e. dc-to-dc converter systems with system coefficients that are piecewise constant in time.

The *State Space Averaging Modelling Method* was developed primarily for calculating the frequency response of constant switching frequency PWM converter systems. There are efforts to extend this method to other classes of converter systems, e.g. current programmed converters[4,5]. It is well known that the method fails to predict the high frequency response of current programmed converter systems[2]. Furthermore, this method does not work on resonant converters.

Sampled-Data Modelling was developed to overcome the problem encountered when using the *State Space Averaging Modelling Method* to calculate the frequency response of current programmed converter systems. This method adds a sampling process and a modulator model to the *State Space Averaging Model* to overcome the problem. However, this method, as with the *State Space Averaging Modelling*, does not work with resonant converters.

Small-Signal Analysis of Resonant Converters was developed primarily for resonant converter systems. This method can predict the low frequency response of most converter systems. However, at *"high frequency"*, i.e. close to half of the switching frequency, the method gives erroneous results. This method always predicts that the phase of the frequency response at a multiple of half the switching frequency of any converter system is a multiple of 180 degrees. It is observed from experiments that this is simply not correct.

Small-Signal Frequency Response Theory is developed to overcome the problems in the modelling methods mentioned above, and the central idea behind the theory is very different. All of the three methods described above are based on an idea called *"averaging"*. A dc-to-dc switching converter system is essentially a sampled-data system in the *small-signal limit*.

This work was conducted under the Power Electronics Program support by grants from the GTE Corporation and Emerson Electric Company, and under a contract from IBM Tucson.

0275-9306/86/0000-0186 $1.00 © 1986 IEEE

"Averaging" is used in these methods to relate the output sequence of the discrete time system embedded in the sampled-data system to the actual continuous output of the system. Instead of using the fuzzy idea of *"averaging"*, *Small-Signal Frequency Response Theory* directly computes the Laplace transform of the perturbed output signal which is determined by the perturbed output sequence of the discrete time system embedded in the converter system. The computation of this Laplace transform is possible in the *small-signal limit* because of the nice mathematical properties of the ideal dc-to-dc converter systems. As a result, *Small-Signal Frequency Response Theory* corresponds to the exact frequency domain linearization of an ideal dc-to-dc converter system. *Small-Signal Frequency Response Theory* does not treat input-to-output frequency response, which is commonly known as audio susceptibility, because the time-varying nature of input-to-output frequency response results in a very complicated response with convolution in the frequency domain. This result is not practical for application. However, useful approximations may be obtained by modelling the input signal appropriately.

This paper is divided into four sections. The first section introduces the ideal dc-to-dc converter system — its properties and its control. The second section discusses the application of *Small-Signal Frequency Response Theory* to a very simple converter system. This section is aimed at providing a geometrical interpretation of the theory before it is introduced in the next section. The third section introduces *Small-Signal Frequency Response Theory* formally for a subset of ideal dc-to-dc converter systems. It starts with a systematic procedure for constructing the difference equation which describes the small-signal motion of the system about a given steady state solution. Then, the *"equivalent hold"* is introduced to relate the output sequence of this difference equation to the continuous output signal. Three different control strategies, namely, PWM, programmed, and bang-bang are used as examples in this section. In each example, the theoretically predicted and experimentally measured Bode plots of the frequency response are presented. Finally, in the fourth section, a systematic procedure for constructing the augmented difference equation that describes the small-signal motion of the system about a given steady state solution for all the ideal dc-to-dc converter system described in the first section is introduced. The *generalized equivalent hold* is also introduced in this section to relate the output of this augmented difference equation to the continuous output signal.

1 Ideal Dc-to-Dc Converter Systems

Real life systems are never ideal. However, in many cases, for the behavior under study, an ideal system model that can approximate the real life system can be found. A real life dc-to-dc converter is not linear, none of the switching devices behaves like an ideal switch, and magnetic components have nonlinearities with memory. Fortunately, for study of its frequency domain behavior, a real life dc-to-dc converter system may be modelled as an ideal converter system. Even in the worst case, the addition of parasitic elements to the model usually gives a satisfactory result. However, an ideal converter system model is usually not sufficient to model the detailed time domain behavior of real life converter systems.

Small-Signal Frequency Response Theory is a mathematical theory for linearization of an ideal dc-to-dc converter system in the frequency domain for a given steady state solution of the system. For a full understanding of *Small-Signal Frequency Response Theory* it is necessary to define an ideal dc-to-dc converter system and to study its properties and their implications. Furthermore, defining converter systems allows easy classification of converter systems. In Section 1.1, ideal dc-to-dc converter systems are defined. The methods to control converter systems is introduced in Section 1.2. The properties of converters and the implications of these properties, which are relevant to *Small-Signal Frequency Response Theory*, are discussed in Section 1.3.

1.1 Definition of Ideal Dc-to-Dc Converter Systems

Ideal dc-to-dc converter systems have many mathematical properties. These properties, in turn, have some implications on how the systems should be handled mathematically. Before discussing the properties of an ideal dc-to-dc converter system, it is necessary to define it mathematically.

An ideal dc-to-dc converter system is described by Eq. (1):

$$\begin{aligned} \dot{\mathbf{x}}(t) &= \mathbf{A}(t)\,\mathbf{x}(t) + \mathbf{B}(t)\,\mathbf{u} \\ \mathbf{y}(t) &= \mathbf{C}(t)\,\mathbf{x}(t) + \mathbf{D}(t)\,\mathbf{u} \end{aligned} \tag{1}$$

where $\mathbf{x}(t)$ is the *state vector*, $\mathbf{u}$ is the *input vector*, $\mathbf{y}(t)$ is the *output vector*, $\mathbf{A}(t)$ is the *system matrix*, $\mathbf{B}(t)$ is the *input matrix*, $\mathbf{C}(t)$ is the *output matrix* and $\mathbf{D}(t)$ is the *transmission matrix*.

$\mathbf{A}(t), \mathbf{B}(t), \mathbf{C}(t)$ and $\mathbf{D}(t)$ have the following properties:

1. $\mathbf{A}(t), \mathbf{B}(t), \mathbf{C}(t)$ and $\mathbf{D}(t)$ are piecewise constant functions in time t, i.e.

   $$(\mathbf{A}(t), \mathbf{B}(t), \mathbf{C}(t), \mathbf{D}(t)) = (\mathcal{A}_i, \mathcal{B}_i, \mathcal{C}_i, \mathcal{D}_i),\ \mathcal{T}_i < t < \mathcal{T}_{i+i}$$

2. The ordered quadruple $(\mathbf{A}(t), \mathbf{B}(t), \mathbf{C}(t), \mathbf{D}(t))$ assumes only a finite set of values, i.e.

   $$(\mathcal{A}_i, \mathcal{B}_i, \mathcal{C}_i, \mathcal{D}_i) \in \{(\mathbf{A}_i^*, \mathbf{B}_i^*, \mathbf{C}_i^*, \mathbf{D}_i^*) : 1 \le i \le N_n\}$$

   where N_n is the *number of switched-networks*.

3. An ideal dc-to-dc converter system is controlled not by its input vectors $\mathbf{u}$, but by varying its $\mathcal{T}_i$'s. (See Section 1.2.) The method that determines $\mathcal{T}_i$, i.e. the modulation method, is $\mathcal{M}_i$.

When an ideal dc-to-dc converter system is operating in steady state, its steady state solution may be characterized by the sequences $\{(\mathbf{A}_i, \mathbf{B}_i, \mathbf{C}_i, \mathbf{D}_i)\}$, $\{\mathbf{T}_i\}$ and $\{M_i\}$. These are the sequences $\{(\mathcal{A}_i, \mathcal{B}_i, \mathcal{C}_i, \mathcal{D}_i)\}$, $\{\mathcal{T}_i\}$ and $\{\mathcal{M}_i\}$, respectively, corresponding to the steady state solution. The following are the properties of these sequences:

1. In steady state, the sequence $\{(\mathbf{A}_i, \mathbf{B}_i, \mathbf{C}_i, \mathbf{D}_i)\}$ is periodic with period N_q, i.e. $\forall i \in \mathbf{Z}$,

   $$(\mathbf{A}_i, \mathbf{B}_i, \mathbf{C}_i, \mathbf{D}_i) = (\mathbf{A}_{i+N_q}, \mathbf{B}_{i+N_q}, \mathbf{C}_{i+N_q}, \mathbf{D}_{i+N_q})$$

   For a system to operate as a converter system, $N_q \ge 2$.

2. In steady state the sequence $\{M_i\}$ is periodic with period N_M, i.e. $M_i = M_{i+N_M}, \forall i \in \mathbf{Z}$.

3. Define: $T_i \equiv \mathbf{T}_{i+1} - \mathbf{T}_i$. The sequence $\{T_i\}$ is periodic with period N_T, i.e. $T_{i+N_T} = T_i$, $\forall i \in \mathbf{Z}$.

4. The *number of switched-states* N_s is defined as:

$$N_s \equiv \mathrm{lcm}(N_q, N_T, N_m)$$

i.e. N_s is the least common multiplier of N_q, N_T, and N_m. For most common converters the *number of switched-states* is the same as the number of switched-networks.

For the system to be linearizable, it is necessary that in the presence of *small* perturbations, (especially in the *small-signal limit*), $\{(\mathcal{A}_i, \mathcal{B}_i, \mathcal{C}_i, \mathcal{D}_i)\} = \{(\mathbf{A}_i, \mathbf{B}_i, \mathbf{C}_i, \mathbf{D}_i)\}$ and $\{\mathcal{M}_i\} = \{\mathbf{M}_i\}$.

1.2 The Control of Ideal Dc-to-Dc Converter Systems

Dc-to-dc converter systems, as discussed in Section 1.1, are not controlled by the input vector $\mathbf{u}$. The input vector usually represents the power sources. If the power source can be varied to control the dc-to-dc converter system, the converter system is unnecessary. In most cases, the variations in the input vector $\mathbf{u}$ are regarded as disturbances. Dc-to-dc converter systems are controlled by changing the $\mathcal{T}_i$'s defined as in Section 1.1. There are four major classes of modulation methods that determine the $\mathcal{T}_i$'s. Define: $\Delta t_i \equiv \mathcal{T}_i - \mathbf{T}_i$. In the *small-signal limit*, Δ becomes δ; e.g. Δt_i becomes δt_i. The four major modulation methods may be described as follows:

1. *Unmodulated* — the Δt_i's corresponding to this method are zero, i.e. $\Delta t_i \equiv 0$, $\forall i \in \{i \mid \mathcal{M}_i = \mathcal{M}^u\}$. The superscript u is used to denote that the quantity corresponds to the unmodulated case.

2. *Time-Modulated* — the Δt_i's corresponding to this modulation method are determined by a sequence in the following manner: $\Delta t_i = (m_i^t)^{-1} \Delta r_i$, $\forall i \in \{i \mid \mathcal{M}_i = \mathcal{M}^t\}$ where Δr_i is a sequence and m_i^t is the slope of the PWM ramp. The superscript t is used to denote that the quantity corresponds to the time-modulated case. If $\Delta r_i = \Delta r(\mathcal{T}_i)$ for some signal $\Delta r(t)$, then Δr is naturally sampled. If $\Delta r_i = \delta r(\mathbf{T}_i + c)$ for some signal $\Delta r(t)$ and constant c, then Δr is uniformly sampled. In this paper, c is assumed to be zero. It turns out that these two sampling methods do not make a difference in the result given by *Small-signal Frequency Response Theory* for $c = 0$.

3. *Constraint-Modulated* — better known as programming. The Δt_i's corresponding to this modulation method satisfy the following constraint equation:

$$\mathbf{f}^T \mathbf{x}(\mathbf{T}_i + \Delta t_i) - r(\mathbf{T}_i + \Delta t_i) + m^c \Delta t_i + c = 0$$

$\forall t$ such that $\mathcal{T}_{i-1} < t < \mathcal{T}_{i+1}$ and $\forall i \in \{i \mid \mathcal{M}_i = \mathcal{M}^c\}$, where $\mathbf{f}$ is a vector, $r(t)$ is the control signal, and m^c is the slope of the added ramp. The superscript c is used to denote that the quantity corresponds to the constraint-modulated case. This constraint equation can be linearized in the small-signal limit to:

$$\mathbf{f}^T \dot{\mathbf{x}}^-(\mathcal{T}_i)\, \delta t_i + \mathbf{f}^T \delta x(\min(\mathbf{T}_i, \mathcal{T}_i)) - \delta r(\mathcal{T}_i) + m^c \delta t_i = 0$$

4. *Modified-Time-Modulated* — this modulation method appears commonly in constant on/off time converters and frequency modulated resonant converters. In this case, $\Delta t_i = m^{m-1} \Delta r_i + h \Delta t_{i-1}$, $\forall i \in \{i \mid \mathcal{M}_i = \mathcal{M}^m\}$. The superscript m is used to denote that the quantity corresponds to the modified-time-modulated case.

For example, a bang-bang controlled converter is not a fixed switching frequency converter. In general, for any converter system operating with fixed switching frequency, M^u must be in the sequence $\{M_i\}$. For a two switched-state bang-bang controlled converter system, $N_M = 1$ and all the transitions are constraint modulated. $N_T = 2$ and $N_q = 2$, $N_s = lcm(1,2,2) = 2$. A bang-bang controlled converter is a simple sliding mode controlled converter.

1.3 Properties of Ideal Dc-to-Dc Converter Systems

In order to understand the ideal dc-to-dc converter problem, the properties of ideal dc-to-dc converter systems must be studied. Many of the properties of ideal dc-to-dc converter systems are stated in Section 1.1. The properties that are of greatest interest are the following:

- The system is described by a linear differential equation at any instant of time except at $\mathcal{T}_i$, the instants of switching.
- The differential equation has *'piecewise constant coefficients'* in time.
- The switching time is zero.
- Nonlinearity comes from switching.
- The switching frequency is finite.
- The system state vector is continuous in time.
- The system output vector may be discontinuous in time.

These properties imply that a solution to the system exists at all times and, given the control $r(t)$ and the initial condition, the output waveform can be computed. *Small-Signal Frequency Response Theory* makes use of the fact that the output waveform can be computed to its full advantage and takes account of finite switching frequency.

2 A Simple Example Converter System

Consider the circuit shown in Fig. 1, a current programmed buck converter. When a sufficiently large output capacitor with very low ESR is used and inductor current is the only concern, the circuit shown in Fig. 2 can be used to model this converter circuit. In the following sections, the steady state operation and the motion of this converter circuit will be studied in detail. Since the interest in this discussion is the inductor current only, the circuit shown in Fig. 2 will be used instead of the circuit shown in Fig. 1 in this study. The steady state solution of this converter system is discussed in Section 2.1. This converter circuit has infinitely many solutions for a given operating condition. In Section 2.2, the motion of the system is studied using a difference equation. The concept of stability for converters in will be introduced. In Section

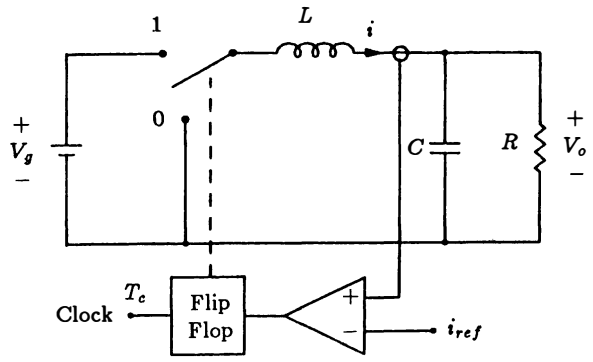

Fig. 1: Current-programmed buck converter.

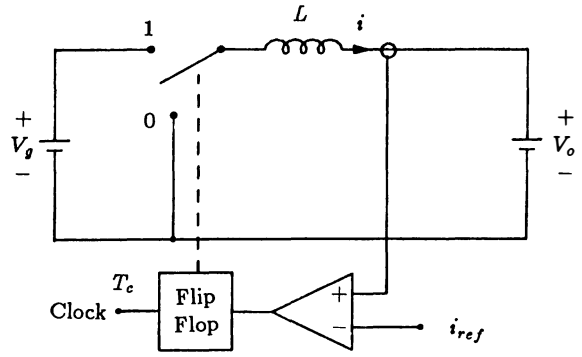

Fig. 2: Circuit model for inductor current calculation of the converter circuit shown in Fig. 1.

2.3, the link between the difference equation and the frequency response of the converter is established. The basic concepts of *Small-Signal Frequency Response Theory* are those which are introduced through Sections 2.2 and 2.3. This introduction to the theory through a simple example is aimed at providing an understanding and a geometrical interpretation of the theory.

2.1 The Steady State of the System

The steady state solution of the converter system shown in Fig. 2 can be easily calculated. The quantity of interest in this study is the inductor current i. The state equation of the system for the switch in position 0 is:

$$\frac{di}{dt} = -\frac{V_o}{L} \tag{2}$$

and for the switch in position 1 is:

$$\frac{di}{dt} = \frac{V_g - V_o}{L} \tag{3}$$

The description of the converter in the framework of Section 1 is:

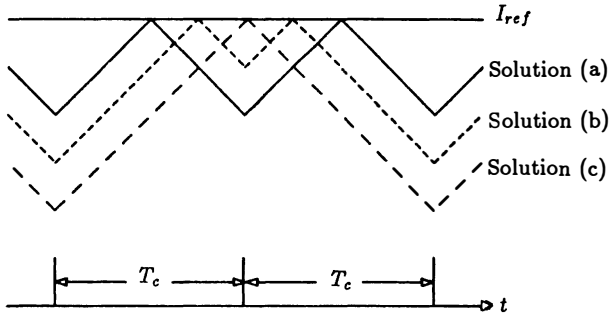

Fig. 3: Three steady state solutions of the inductor current for a given operating condition of the converter circuit shown in Fig. 2.
(a) $n = 1$, $T_s = T_c$, $N_T = 2$, $N_s = 2$.
(b) $n = 2$, $T_s = 2T_c$, $N_T = 4$, $N_s = 4$.
(c) $n = 1$, $T_s = 2T_c$, $N_T = 2$, $N_s = 2$.

$$\begin{aligned} \mathbf{x}(t) &= i(t) & \mathbf{u} &= \begin{pmatrix} V_g \\ V_o \end{pmatrix} \\ \mathbf{A}_{2i} &= 0 & \mathbf{A}_{2i+1} &= 0 \\ \mathbf{B}_{2i} &= \left(0, -\frac{1}{L}\right) & \mathbf{B}_{2i+1} &= \left(\frac{1}{L}, -\frac{1}{L}\right) \\ N_q &= 2 \end{aligned}$$

In this example, the order of the system is one and the system matrices and the state vector degenerate to scalars. In order to keep the example simple, $\mathbf{x}(t)$ will be used as the output and therefore ignore the $\mathbf{C}$ and $\mathbf{D}$ matrices.

The control of this converter is described below:

$$\begin{aligned} N_M &= 2 \\ M_{2i+1} &= M^u \\ M_{2i} &= M^c \end{aligned}$$

However, it is possible that $N_T = n\,N_M, \forall n \in \mathbf{Z}^+$. There is a degree of freedom – the choice of n, in finding the steady state solution. The steady state solution of the converter system is denoted by $\mathbf{X}(t)$. For a valid steady state solution, the boundary condition on $\mathbf{X}(t)$ is:

$$\mathbf{X}(t) = \mathbf{X}(t + \sum_{j=1}^{N_T} T_j) \tag{4}$$

For $n = 1$, $N_s = 2$, and $T_0 + T_1 = T_s = T_c$, where T_c is the clock period, the waveform of the inductor current is shown in Fig. 3. The slope of the waveform of the current ramping up is:

$$m_1 = \frac{V_g - V_o}{L} \tag{5}$$

The slope of the current ramping down is:

$$m_0 = \frac{-V_o}{L} \tag{6}$$

The boundary condition requires:

$$\begin{aligned} m_0 T_0 + m_1 T_1 &= 0 \\ \Longrightarrow \qquad \frac{T_0}{T_1} &= \frac{V_g - V_o}{V_o} \end{aligned}$$

The steady state duty cycle $D \equiv T_1/(T_0 + T_1) = V_o/V_g$.

For $n = 2$, $N_T = 4$, $N_s = 4$, $T_s = T_0 + T_1 + T_2 + T_3$, and $T_1 + T_2 = T_c$, $T_3 + T_0 = T_c$, the waveform of the inductor current is also shown on Fig. 3. The slope of the waveform is the same as the case for $n = 1$. However, the boundary conditions become:

$$m_0 T_0 = m_1 T_1 \quad (7)$$

$$m_1 T_2 = m_1 T_3 \quad (8)$$

Equation (7) and Eq. (8) with $T_1 + T_2 = T_c$ and $T_3 + T_0 = T_s$ form a system of four linear equations with four unknowns T_0, T_1, T_2, T_3, which can be solved. In general, for $n = k$, there is a system of k linear equations with k unknowns. Therefore, for each $n \in \mathbf{Z}^+$, a steady state solution for this converter system can be found for each given operating condition — V_g and V_o. However, not all of the steady state solutions are stable solutions. Therefore it does not make any sense to use an operating point, a term that is commonly used in electronic circuits, to characterize the steady state solution for this class of converter systems. Any converter using *constraint-modulation* has this problem. This phenomenon is a manifestation of the nonlinearity of converter systems.

Furthermore, from the circuit it is obvious that it is possible that $T_1 + T_2 = nT_s, n \in \mathbf{Z}^+$, provided that $T_1 > (n-1)T_s$. For $T_1 + T_2 = 2T_s$, this phenomenon is also referred to as period doubling, which is quite commonly observed experimentally. (See Fig. 3.) However, not all operating conditions can result in this type of phenomenon. It is also possible to have a hybrid of the phenomena mentioned above.

From the steady steady solution of this simple example converter circuit, one can conclude that:

1. It is not sufficient to characterize the steady state solution of converter circuits with circuit operation parameters such as supply voltage, supply current, reference voltage and reference current.

2. A possible way to specify the steady state solution is to use the circuit parameters and the T_i's.

3. As a result, it is not appropriate to talk about the frequency response of a converter circuit under certain operating conditions. The frequency response of a converter circuit corresponds to a steady state solution.

4. Finding an ideal dc-to-dc converter system model from a dc-to-dc converter circuit includes finding the T_i's.

2.2 The Small-Signal Motion of the System

Before studying the frequency response of the converter system, the motion of the system in the time domain must be studied. The motion of an ideal dc-to-dc converter system is complicated. In general, the large-signal motion of the system can only be studied by simulation. Fortunately, the small-signal motion of the system can be characterized by a difference equation. The sequences in the difference equation represent the sampled control signals and sampled system states. The trajectory of the system between the sample points can always be found. This is a fortunate property of ideal dc-to-dc converter systems.

In this section, the small-signal motion of only one particular steady state solution for the circuit shown in Fig. 2 is discussed. This particular steady state solution is the two-switched-state solution $T_0 + T_1 = T_s$ with no period n-tupling. It is not hard to find the difference equation that describes the small-signal motion of other steady solutions using a geometrical approach.

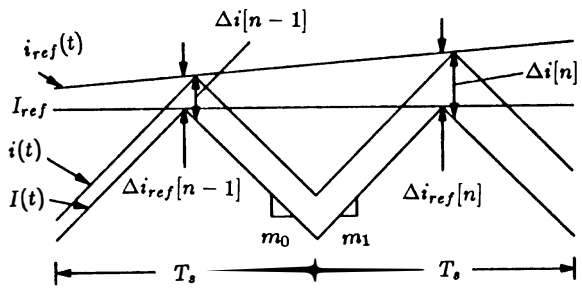

Fig. 4: Steady state inductor current — $I(t)$, perturbed inductor current — $i(t)$, and related definitions.

The steady state solution waveform, i.e. the steady state inductor current waveform, and the perturbed waveform are shown in Fig. 4.

The difference equation that describes the small motion of a n-switched-state converter system about a steady state solution has the function of relating a sample of the system state at a sample point to the sample of the system state at a similar sample point n switched-states earlier and to the control-input sample. From the geometry shown in Fig. 4, one can easily arrive at the following difference equation:

$$\Delta i_0[n] = k\,\Delta i_0[n-1] + (1-k)\,\Delta i_{ref}[n] + O(\Delta^2) \quad (9)$$

where $k \equiv \frac{m_0}{m_1}$. In the em small-signal limit, the difference equation is linear and becomes:

$$\delta i_0[n] = k\,\delta i_0[n-1] + (1-k)\,\delta i_{ref}[n] \quad (10)$$

It is obvious that the small-signal motion of the system is unstable when $k > 1$.

2.3 The Frequency Response of the System

In this section, the frequency response of the output i with respect to the control-input i_{ref} will be studied, where $i(t) = I(t) + \delta i(t)$, $i_{ref}(t) = I_{ref} + \delta i(t)$, in which $I(t)$ is the steady state solution of $i(t)$ and I_{ref} is the controlling reference signal i_{ref} in steady state. Since $I(t)$ is periodic with period T_s, the switching period, it does not contribute to the frequency response. The steady state reference current I_{ref} is a dc quantity; it does not contribute to the frequency response. Therefore, the frequency response of i with respect to i_{ref} is the same as the frequency response of δi with respect to δi_{ref} in the *small-signal limit*.

In Section 2.1, the difference equation, Eq. (9), which describes the relation between $\delta i_0[n]$ and $\delta i_0[n-1]$ is derived. To find the small-signal frequency domain relation between i and i_{ref}, the following three links must be established:

1. Given $\delta i_{ref}(s)$, the Laplace transform of $\delta i_{ref}(t)$, find

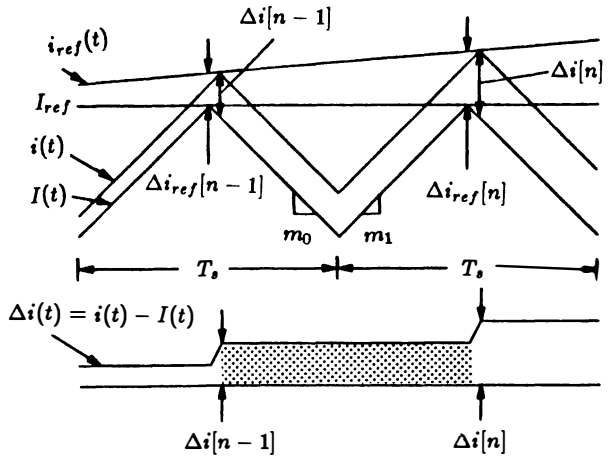

Fig. 5: Contribution of $\Delta i_0[n]$ to $\Delta i(t)$ — shaded area.

$\delta i^*_{ref}(s)$, the Laplace transform of the sampled $\delta i_{ref}(t)$.

$$\delta i^*_{ref}(s) \equiv \mathcal{L}\left\{\sum_n i_{ref}(nT_s)\,\delta(t-nT_s)\right\}$$

2. Given $\delta i^*_{ref}(s)$, find $\delta i^*_0(s)$, the Laplace transform of the sampled $\delta i(t)$.

$$\delta i^*_0(s) \equiv \mathcal{L}\left\{\sum_n i_0[n]\,\delta(t-nT_s)\right\}$$

3. Given $\delta i_0[n]$, find its effect on $\delta i(t)$ and $\delta i(s)$.

The first link is established by Shannon's *Sampling Theorem*[6].

$$\delta i^*_{ref}(s) = \frac{1}{T_s}\sum_n \delta i_{ref}(s + in\omega_s) \tag{11}$$

where $\omega_s = \frac{2\pi}{T_s}$. However, there is a complication, which is that i_{ref} may be naturally sampled, i.e. not uniformly sampled. Fortunately, it may be shown that the effect of this *almost periodic sampling* is merely the introduction of noise to the system in the *small-signal limit.*

The second link is the z-transform[7]. Applying the z-transform to the difference equation, Eq. (9), it becomes:

$$\delta i(z) = z^{-1}k\delta i(z) + (1-k)\delta i_{ref}(z) \tag{12}$$

Substituting e^{sT_s} for z, then, $i(z) \rightarrow i^*(s)$ and $i_{ref}(z) \rightarrow i^*_{ref}(s)$, and Eq. (12) becomes:

$$\delta i^*(s) = \frac{1-k}{1-ke^{-sT_s}}\, i^*_{ref}(s) \tag{13}$$

The third link is one of the major features of *Small-Signal Frequency Response Theory* which makes it different from other modelling methods. While most other methods use a concept called *averaging* to achieve this, *Small Signal Frequency Response Theory* computes, first, the time domain effect of $\delta i_0[n]$ on the $\delta i(t)$, and then, from the time domain effect, computes the frequency domain effect.

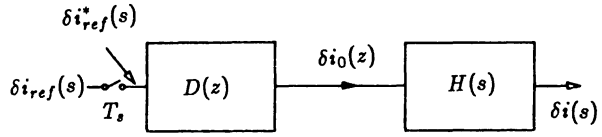

$$k = \frac{m_1}{m_1} \qquad D(z) = (1-kz^{-1})^{-1}(1-k) \qquad H(s) = \frac{1-e^{-sT_s}}{s}$$

Fig. 6: The equivalent linear system for the converter circuit shown in Fig. 2.

Figure 5 shows the time domain effect of $\Delta i_0[n]$ on the $\Delta i(t)$. The shaded area under the waveform of $\Delta i(t)$ is the influence of $\Delta i_0[n]$ on $\Delta i(t)$. In the *small-signal limit*, $\delta i_{ref} \rightarrow 0$, $\Delta i_0[n] \rightarrow \delta i_0[n]$ and $\Delta i(t) \rightarrow \delta i(t)$. The trapezoidal areas under the waveform approach zero much faster than the rectangular areas in the *small-signal limit* and therefore can be neglected for small-signal calculation. The effect of $\delta i_0[n]$ on $\delta i(t)$ is a rectangular piece of the waveform of *'length'* in time T_s, and *'height'* of $\delta i_0[n]$. This shaded part in the *small-signal limit* is exactly the same as the output of the *zero-order-hold*[7] with a δ-function input of magnitude $\delta i_0[n]$. The third link is therefore a *zero-order-hold* and may be described by:

$$\delta i(s) = \frac{1-e^{-sT}}{s}\delta i^*_0(s) \tag{14}$$

The relationship between the spectrum of the output δi and the spectrum of the control-input δi_{ref} can therefore be described by a sampled-data system, shown in Fig. 6. The overall result is:

$$\delta i(s) = G(s)\,\delta i^*_{ref}(s) \tag{15}$$

where

$$\delta i^*_{ref}(s) = \frac{1}{T_s}\sum_n \delta i_{ref}\left(s + \frac{2n\pi}{T_s}\right)$$

$$G(s) = \frac{1-e^{-sT}}{s}\,\frac{1-k}{1-ke^{-sT_s}}$$

Equation (15) is the frequency response of δi with respect to δi_{ref}. The ratio $\delta i(s)/\delta i_{ref}(s)$ may be loosely referred to as the *"transfer function"* from i_{ref} to i, and $G(s)$ is the pulse transfer function.

3 Simple Two-Switched-State Converters

Most of the converters in common use have two switched-networks. In the example converter in Section 2, it was found that even though the converter has only two switched-networks, it may have an unlimited number of switched-states. However, in most cases, one would like to operate the converter such that the number of switched-states is the same as the number of switched-networks. Therefore, the discussion of this section concentrates on two switched-state converters. Furthermore, in this section, both the case of modified-time-modulation and the output equation of the converter system will not be discussed; i.e. ignore **C** and **D**. These topics are discussed in Section 4.

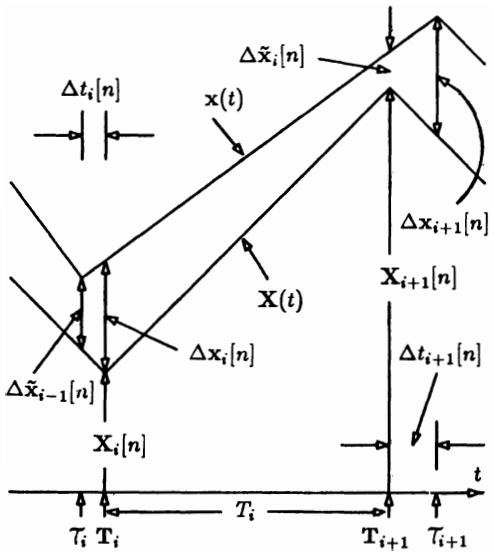

Fig. 7: Steady state state vector $\mathbf{X}(t)$*, perturbed state vector* $\mathbf{x}(t)$*, and related definitions.*

Given an ideal dc-to-dc converter system and its steady state solution, *Small-Signal Frequency Response Theory* gives the control to output frequency response of the system provided that steady state solution is small-signal stable. *Small-Signal Frequency Response Theory* does not tell anything about the steady state solution. Therefore, in the following sections, the steady state solution $\mathbf{X}(t)$ is assumed to be known. The steady state solution $\mathbf{X}(t)$ is periodic with period $T_s = T_0 + T_1$, where T_s is the switching period. For the convenience of describing the problem, define:

$$\mathbf{X}_i \equiv \mathbf{X}(\mathbf{T}_i[n]) \quad (16)$$
$$\Delta\mathbf{x}(t) \equiv \mathbf{x}(t) - \mathbf{X}(t) \quad (17)$$
$$\Delta t_j \equiv \mathcal{T}_j - \mathbf{T}_j \quad (18)$$
$$\Delta t_i[n] \equiv \Delta t_{i+nN_s} \quad (19)$$
$$\Delta\mathbf{x}_j \equiv \Delta\mathbf{x}(\mathbf{T}_j + \max(\delta t_j, 0)) \quad (20)$$
$$\Delta\mathbf{x}_i[n] \equiv \Delta\mathbf{x}_{i+nN_s} \quad (21)$$
$$\Delta\tilde{\mathbf{x}}_j \equiv \Delta\mathbf{x}(\mathbf{T}_{j+1} + \min(\Delta t_{j+1}, 0)) \quad (22)$$
$$\Delta\tilde{\mathbf{x}}_i[n] \equiv \Delta\tilde{\mathbf{x}}_{i+nN_s} \quad (23)$$

These definitions are depicted in Fig. 7.

The steps for finding the frequency response of an ideal two-switched-states dc-to-dc converter system are the same as those used for the simple example converter in Section 2. The first step is to find the difference equation that describes the small-signal system motion. Without loss of generality, only the case of modulating $\Delta t_0[n]$ is considered. This step is discussed in Section 3.1. The next step is to find the *equivalent hold* that links the $\Delta\mathbf{x}_j$'s to $\Delta x(s)$. This step is discussed in Section 3.2.

Following Section 3.2 are three examples of two-switched-state converters, each with a different control strategy. These three control strategies are:

1. Constant switching frequency, time-modulation (PWM) control.
2. Constant switching frequency, constraint-modulation control (programming).
3. Variable switching frequency, bang-bang control.

For each example control strategy, the general results are discussed first and then these results are used to predict the frequency response of an example converter circuit. Experimental results will be compared to the theoretical prediction. The example converter circuit topology used in all three examples is the simple R-L topology. This topology is chosen for the following reasons. First, its steady state can be calculated analytically. Second, it is a first order system with only one reactive element. Therefore, the result is relatively simple. Third, this converter is so simple that parasitics can be neglected or absorbed into its circuit elements. As a result, there is a very good control over the experiments on the circuit. Fourth, this simple topology with the different control strategies can illustrate where the other popular modelling methods fail.

3.1 The Small-Signal Motion

The small-signal motion of an ideal dc-to-dc converter system about a steady state solution may be described by a difference equation that relates $\delta\mathbf{x}_0[n-1]$ to $\delta\mathbf{x}_0[n]$. This difference equation is sufficient to describe the motion of the system because the differential equation that describes the converter system has piecewise constant coefficients in time. As a result of this special form of nonlinearity, the exact trajectory of the system between the sample points given by the difference equation can be found always. Furthermore, if the sequence $\{\delta\mathbf{x}_i\}$ is finite, $\delta\mathbf{x}(t)$ is finite; i.e. the stability of the difference equation implies the small-signal stability of the system.

Before deriving the difference equation that describes the small-signal motion of the system, let us first describe the converter system and its steady state solution in the framework described in Section 1. For a two switched-state converter system in steady state, $\forall i \in \mathbf{Z}$:

$$(\mathbf{A}_{2i}, \mathbf{B}_{2i}, \mathbf{C}_{2i}, \mathbf{D}_{2i}) = (\mathbf{A}_0, \mathbf{B}_0, \mathbf{C}_0, \mathbf{D}_0) \quad (24)$$
$$(\mathbf{A}_{2i+1}, \mathbf{B}_{2i+1}, \mathbf{C}_{2i+1}, \mathbf{D}_{2i+1}) = (\mathbf{A}_0, \mathbf{B}_0, \mathbf{C}_0, \mathbf{D}_0) \quad (25)$$
$$M_{2i} = M_0 \quad (26)$$
$$M_{2i+1} = M_1 \quad (27)$$
$$T_{2i} = T_0 \quad (28)$$
$$T_{2i+1} = T_1 \quad (29)$$

For the converter to be linearizable, the following must hold for the converter perturbed about the steady state solution in the *small-signal limit*:

$$\{(\mathcal{A}_i, \mathcal{B}_i, \mathcal{C}_i, \mathcal{D}_i)\} = \{(\mathbf{A}_i, \mathbf{B}_i, \mathbf{C}_i, \mathbf{D}_i)\} \quad (30)$$
$$\{\mathcal{M}_i\} = \{M_i\} \quad (31)$$

Modulation method M_i determines $\mathcal{T}_i$, i.e. the time of the transition from $(\mathbf{A}_{i-1}, \mathbf{B}_{i-1}, \mathbf{C}_{i-1}, \mathbf{D}_{i-1})$ to $(\mathbf{A}_i, \mathbf{B}_i, \mathbf{C}_i, \mathbf{D}_i)$. Without loss of generality, one can consider M_{2i} to be those that are modulated. The effect of modulating M_{2i+1}'s may be taken into account later by superposition. Define $\tilde{\mathbf{\Phi}}_i, \tilde{\mathbf{K}}_i, \tilde{\mathbf{k}}_i$ by

the following equations:

$$\delta \mathbf{x}_i[n] = \tilde{\mathbf{\Phi}}_i \, \delta \tilde{\mathbf{x}}_i[n] \quad (32)$$

$$\delta \mathbf{x}_i[n] = \tilde{\mathbf{K}}_i \, \delta \tilde{\mathbf{x}}_{i-1}[n] + \tilde{\mathbf{k}}_i \, \delta r_i[n] \quad (33)$$

where $\delta r_i[n]$ is the control-input. There is a different $\tilde{\mathbf{K}}$ and a different $\tilde{\mathbf{k}}$ corresponding to each modulation method.

3.1.1 Unmodulated Transitions

For the unmodulated case where $M_i = M^u$, $\tilde{\mathbf{k}}_i^u = \mathbf{0}$, obviously. The state $\mathbf{x}(t)$ is continuous and $\delta t_i \equiv 0$. Therefore, $\mathbf{x}_i[n] = \tilde{\mathbf{x}}_{i-1}[n]$. As a result, $\tilde{\mathbf{K}}_i^u \equiv \mathbf{I}$.

3.1.2 Time-Modulated Transitions

Consider next the time-modulated case where $M_i = M^t$. The modulating control-input is $\delta r_i[n]$. If the slope of the ramp of the sawtooth wave used in the pulse width modulator is m_i^t, then:

$$\delta t_i[n] = (m_i^t)^{-1} \delta r_i[n] \quad (34)$$

The next step is to express $\delta \mathbf{x}_i[n]$ in terms of $\delta \tilde{\mathbf{x}}_{i-1}[n]$ and $\delta r_i[n]$. From the geometry shown in Fig. 7, it is obvious that:

$$\Delta \mathbf{x}_i[n] = \Delta \tilde{\mathbf{x}}_i[n-1] + \bar{\mathbf{k}}_i \, \Delta t_i[n] + \mathrm{O}(\Delta^2) \quad (35)$$

where

$$\bar{\mathbf{k}}_i \equiv \dot{\mathbf{X}}_i^- - \dot{\mathbf{X}}_i^+$$

$$\dot{\mathbf{X}}_i^- = \mathbf{A}_{i-1} \mathbf{X}_i + \mathbf{B}_{i-1} \mathbf{u}$$

$$\dot{\mathbf{X}}_i^+ = \mathbf{A}_i \mathbf{X}_i + \mathbf{B}_i \mathbf{u}$$

In the *small-signal limit*:

$$\delta \mathbf{x}_i[n] = \delta \tilde{\mathbf{x}}_i[n-1] + (m_i^t)^{-1} \bar{\mathbf{k}}_i \, \delta r_i[n] \quad (36)$$

Therefore:

$$\tilde{\mathbf{K}}_i^t = \mathbf{I} \quad (37)$$

$$\tilde{\mathbf{k}}_i^t = (m_i^t)^{-1} \bar{\mathbf{k}}_i = (m_i^t)^{-1} \{(\mathbf{A}_{i-1} - \mathbf{A}_i)\mathbf{X}_i + (\mathbf{B}_{i-1} - \mathbf{B}_i)\mathbf{u}\} \quad (38)$$

3.1.3 Constraint-Modulated Transitions

For the case of constraint-modulation, $M_i = M^c$, the first step is to find $\delta t_i[n]$ in terms of $\delta \tilde{\mathbf{x}}_{i-1}[n]$ and $\delta r_i[n]$. The constraint equation is:

$$\mathbf{f}_i^T \mathbf{x}\,(\mathbf{T}_{i+nN_s} - \Delta t_i[n]) + m_i^c \, \Delta t_i[n] + c_i - r_i\,(\mathbf{T}_{i+nN_s} - \Delta t_i[n]) = 0 \quad (39)$$

where, $\mathbf{f}_i^T$ is a vector constant and c_i is a scalar constant corresponding to M_i; r_i is the modulating control-input; m_i^c is a constant which is usually the slope of the ramp of the sawtooth wave used in the pulse width modulator, in the case of a PWM converter, and the slope of the added stabilization ramp, in the case of a programmed converter. The constraint equation is the mathematical model of a comparator. If Eq. (39) is perturbed and the steady state part is subtracted out, in the *small-signal limit,* the equation becomes:

$$\mathbf{f}_i^T \, \delta \tilde{\mathbf{x}}_i[n-1] + \mathbf{f}_i^T \dot{\mathbf{X}}_i^- \, \delta t_i[n] + m_i^c \, \delta t_i[n] - \delta r_i[n] = 0 \quad (40)$$

where $\dot{\mathbf{X}}_i^- = \mathbf{A}_{i-1} \mathbf{X}_i + \mathbf{B}_{i-1} \mathbf{u}$ and $\delta r_i[n] \equiv \delta r(\mathbf{T}_{i+nN_s} + \delta t_i[n])$. The next step is to express $\delta t_i[n]$ in terms of the other quantities in the equation:

$$\delta t_i[n] = -\mathbf{p}_i^T \, \delta \tilde{\mathbf{x}}_i[n-1] + m_i \, \delta r_i[n] \quad (41)$$

where

$$\mathbf{p}_i = \left(\mathbf{f}_i^T \dot{\mathbf{X}}_i^- + m_i^c\right)^{-1} \mathbf{f}_i$$

$$m_i = \left(\mathbf{f}_i^T \dot{\mathbf{X}}_i^- + m_i^c\right)^{-1}$$

With use of this result and the result of the time-modulated case, then:

$$\delta \mathbf{x}_i[n] = \left(\tilde{\mathbf{K}}_i^t - \bar{\mathbf{k}}_i \, \mathbf{p}_i^T\right) \delta \tilde{\mathbf{x}}_{i-1}[n] + m_i \, \bar{\mathbf{k}}_i \, \delta r_i[n] \quad (42)$$

Therefore:

$$\tilde{\mathbf{K}}_i^c = \tilde{\mathbf{K}}_i^t - \bar{\mathbf{k}}_i \, \mathbf{p}_i^T \quad (43)$$

$$\tilde{\mathbf{k}}_i^c = m_i \, \bar{\mathbf{k}}_i \quad (44)$$

3.1.4 Between the Transitions

The $\tilde{\mathbf{\Phi}}_i$'s are relatively easy to find. Consider the differential equation that describes $\Delta \mathbf{x}(t)$ for for time t such that $\max(T_i, \tau_i) < t < \min(T_{i+1}, \tau_{i+1})$:

$$\Delta \dot{\mathbf{x}}(t) = \dot{\mathbf{x}}(t) - \dot{\mathbf{X}}(t) = \mathbf{A}_i \, \Delta \mathbf{x}(t) \quad (45)$$

The solution to this equation is:

$$\Delta \mathbf{x}(t) = e^{\mathbf{A}_i (t - \tau_i)} \mathbf{x}(\tau_i), \qquad \tau_i < t < \tau_{i+1} \quad (46)$$

Therefore, in the *Small-Signal Limit*:

$$\delta \tilde{\mathbf{x}}_i[n] = e^{\mathbf{A}_i T_i} \delta \mathbf{x}_i[n] \quad (47)$$

$$\tilde{\mathbf{\Phi}}_i = e^{\mathbf{A}_i T_i} \quad (48)$$

3.1.5 The Difference Equation

After finding the $\tilde{\mathbf{\Phi}}_i$'s, $\tilde{\mathbf{K}}_i$'s, and $\tilde{\mathbf{k}}_i$'s, the next step is to construct the difference equation. As was mentioned before, it is assumed that M_{2j} only is being modulated The difference equation is:

$$\begin{aligned} \delta \mathbf{x}_0[n] &= \tilde{\mathbf{K}}_0 \, \delta \tilde{\mathbf{x}}_1[n-1] + \tilde{\mathbf{k}}_0 \, \delta r_0[n] \\ &= \tilde{\mathbf{K}}_0 \tilde{\mathbf{\Phi}}_1 \, \delta \mathbf{x}_1[n-1] + \tilde{\mathbf{k}}_0 \, \delta r_0[n] \\ &= \tilde{\mathbf{K}}_0 \tilde{\mathbf{\Phi}}_1 \tilde{\mathbf{K}}_1 \, \delta \tilde{\mathbf{x}}_0[n-1] + \tilde{\mathbf{k}}_0 \, \delta r_0[n] \\ &= \tilde{\mathbf{K}}_0 \tilde{\mathbf{\Phi}}_1 \tilde{\mathbf{K}}_1 \tilde{\mathbf{\Phi}}_0 \, \delta \mathbf{x}_0[n-1] + \tilde{\mathbf{k}}_0 \, \delta r_0[n] \end{aligned} \quad (49)$$

For convenience, define the following quantities:

$$\tilde{\mathbf{\Phi}} = \tilde{\mathbf{K}}_0 \tilde{\mathbf{\Phi}}_1 \tilde{\mathbf{K}}_1 \tilde{\mathbf{\Phi}}_0 \quad (50)$$

$$\tilde{\mathbf{k}} = \tilde{\mathbf{k}}_0 \quad (51)$$

Then, the difference equation that describes the small-signal motion of the system is:

$$\delta \mathbf{x}_0[n] = \tilde{\mathbf{\Phi}} \, \delta \mathbf{x}_0[n-1] + \tilde{\mathbf{k}} \, \delta r_0[n] \quad (52)$$

For the system to be *small-signal stable* about a steady state solution, the difference equation that describes its motion about the steady state solution must be stable. For the difference equation to be stable, all the eigenvalues of $\tilde{\mathbf{\Phi}}$ must lie on the unit disk, i.e. $\max \mid \lambda(\tilde{\mathbf{\Phi}}) \mid \leq 1$.

3.2 The Frequency Response

As was mentioned in Section 2, three links are needed to find the frequency response of the system. The three links are: the relationship between $\delta r_0(t)$ and $\delta r_0[n]$; the frequency domain relation between the sequences of δ-functions with magnitude $\{\delta r_0[n]\}$ and $\{\delta \mathbf{x}_0[n]\}$; and the effect of $\delta \mathbf{x}_i[n]$ on $\delta \mathbf{x}(t)$ and therefore $\delta \mathbf{x}(s)$. As discussed in Section 2, the first link is given by Shannon's *Sampling Theorem* and the second link is given by the *z-transform* of the difference equation that describes the small-signal motion of the system and then substitutes e^{sT_s} for z. The only link that has to be worked on is the effect of $\delta \mathbf{x}_i[n]$ on $\delta \mathbf{x}(s)$.

The differential equation that describes $\delta \mathbf{x}(t)$ is given below:

$$\delta \dot{\mathbf{x}}(t) = \mathbf{A}_i \, \delta \mathbf{x}(t) \tag{53}$$

for $\max(T_j, \mathcal{T}_j) < t < \min(T_{j+1}, \mathcal{T}_{j+1})$, where, $j = i + nN_s$. There are instants in time for which $\delta \mathbf{x}(t)$ is not described by this equation. However, the length of these instants is of the order of δt and therefore $\delta \mathbf{x}(t)$ during these instants has a negligible contribution to $\delta \mathbf{x}(s)$ in the *small-signal limit.*

To find out the *equivalent hold* that relates $\delta \mathbf{x}_i[n]$ to $\delta \mathbf{x}(s)$, the Laplace transform is applied to Eq. (53) for time t, such that $\max(T_j, \mathcal{T}_j) < t < \min(T_{j+1}, \mathcal{T}_{j+1})$.

$$\int_{\max(T_j,\mathcal{T}_j)}^{\min(T_{j+1},\mathcal{T}_{j+1})} \delta \dot{\mathbf{x}}(t)\, e^{-st}\, dt = \mathbf{A}_i \int_{\max(T_j,\mathcal{T}_j)}^{\min(T_{j+1},\mathcal{T}_{j+1})} \delta \mathbf{x}(t)\, e^{-st}\, dt \tag{54}$$

After manipulation and taking the *small-signal limit,* this equation becomes:

$$\begin{aligned} \delta \mathbf{x}'(s) &= [s\mathbf{I} - \mathbf{A}_i]^{-1} \left(e^{-s\mathbf{T}_i}\, \delta \mathbf{x}_i[n] - e^{-s\mathbf{T}_{i+1}}\, \delta \tilde{\mathbf{x}}_i[n] \right) \right) \\ &= e^{-s\mathbf{T}_i} [s\mathbf{I} - \mathbf{A}_i]^{-1} \left[\mathbf{I} - e^{-sT_i}\, e^{\mathbf{A}_i T_i} \right] \delta \mathbf{x}_i[n] \end{aligned} \tag{55}$$

where $\delta \mathbf{x}'(s)$ is the effect of $\delta \mathbf{x}_i[n]$ on $\delta \mathbf{x}(s)$. Therefore, the *equivalent hold* for $\{\delta \mathbf{x}_i[n]\}$ with fixed i is:

$$\tilde{\mathbf{H}}_i(s) = [s\mathbf{I} - \mathbf{A}_i]^{-1} \left[\mathbf{I} - e^{-sT_i}\, e^{\mathbf{A}_i T_i} \right] \tag{56}$$

Putting all the results in this section together and following the strategy for obtaining the frequency response laid out in Section 2, then:

$$\begin{aligned} \delta \mathbf{x}(s) &= \left\{ \tilde{\mathbf{H}}_0(s) + e^{-sT_0}\, \tilde{\mathbf{H}}_1(s)\, \tilde{\mathbf{K}}_1\, \tilde{\mathbf{\Phi}}_0 \right\} \\ &\quad \cdot \left\{ \mathbf{I} - e^{-sT_s}\, \tilde{\mathbf{\Phi}} \right\}^{-1} \tilde{\mathbf{k}}\, \delta r_0^*(s) \end{aligned} \tag{57}$$

where

$$\delta r_0^*(s) = \frac{1}{T_s} \sum_{n=-\infty}^{\infty} \delta r_0(s + \frac{i2n\pi}{T_s})$$

Equation (57) describes the *small-signal frequency response* of a simple ideal two-switched-state dc-to-dc converter system.

3.3 Constant Frequency PWM Converters

With use of the framework for describing ideal converters discussed above, a constant switching frequency pulse-width-modulated (PWM) converter is described by $M_{2i} = M^t$ and $M_{2i+1} = M^u$. Note that for any converter to be operating at constant switching frequency, $M^u \in \{M_i\}$.

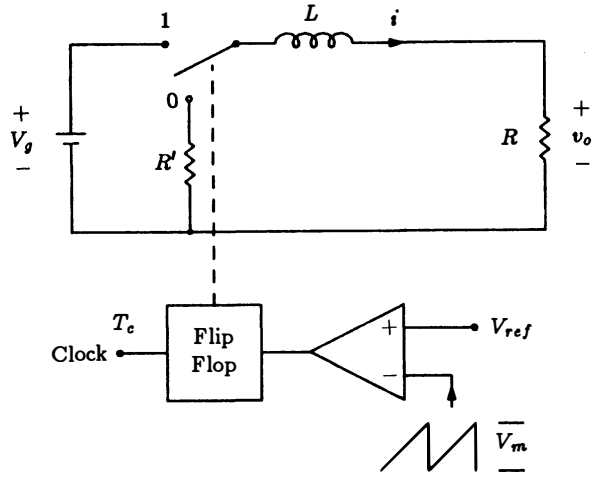

Fig. 8: A constant switching frequency PWM R-L converter: $V_g = 15$Volts, $L = 1.41$mH, $R = 56\Omega$, $R' = 0\Omega$, $T_s = T_c = 20$kHz.

From Eq. (57), the frequency response of the PWM converter system with control-input r_0 is:

$$\begin{aligned} \delta \mathbf{x}(s) &= \left\{ \tilde{\mathbf{H}}_0(s) + e^{sT_0}\, \tilde{\mathbf{H}}_1(s)\, e^{\mathbf{A}_0 T_0} \right\} \\ &\quad \cdot \left\{ \mathbf{I} - e^{-sT_s}\, e^{\mathbf{A}_1 T_1}\, e^{\mathbf{A}_0 T_0} \right\}^{-1} \tilde{\mathbf{k}}\, \delta r_0^*(s) \end{aligned} \tag{58}$$

where

$$\begin{aligned} \tilde{\mathbf{H}}_i(s) &= [s\mathbf{I} - \mathbf{A}_i]^{-1} \left[\mathbf{I} - e^{-sT_i}\, e^{\mathbf{A}_i T_i} \right] \\ \tilde{\mathbf{k}} &= m_0^{t\,-1} \{ (\mathbf{A}_1 - \mathbf{A}_0)\, \mathbf{X}_0 + (\mathbf{B}_1 - \mathbf{B}_0)\, \mathbf{u} \} \end{aligned}$$

In the high switching frequency limit, i.e. $1/T_s \to \infty$ or $T_s \to 0$, then $\tilde{\mathbf{H}}_i(s) \to T_i \mathbf{I}$, $\delta r_0^*(s) \to \delta r_0(s)/T_s, \mathbf{X}_0 \to \mathbf{X}$, and Eq. (58) becomes:

$$\begin{aligned} \lim_{T_s \to 0} \delta \mathbf{x}(s) &= \left\{ sI - (\frac{T_0}{T_s}\mathbf{A}_0 + \frac{T_1}{T_s}\mathbf{A}_1 T_1) \right\}^{-1} \tilde{\mathbf{k}}\, \frac{1}{T_s} \delta r_0(s) \\ &= \{ s\mathbf{I} - \mathbf{A} \}^{-1} \\ &\quad \cdot \{ (\mathbf{A}_1 - \mathbf{A}_0)\, \mathbf{X}_0 + (\mathbf{B}_1 - \mathbf{B}_0)\, \mathbf{u} \} \frac{\delta r_0(s)}{m_0^t T_s} \end{aligned} \tag{59}$$

where $\mathbf{A} \equiv \frac{T_0}{T_s}\mathbf{A}_0 + \frac{T_1}{T_s}\mathbf{A}_1$. The quantities D_0 and D_1 are commonly known as duty ratios. One can identify $\delta r_0(s)/(m_0^t T_s)$ with the $\hat{d}(s)$, $\frac{T_1}{T_s}$ with D, the duty ratio, $\frac{T_0}{T_s}$ with D', $\delta \mathbf{x}(s)$ with $\hat{\mathbf{x}}(s)$, used in the literature on *State Space Averaging Modelling Method*[1,4,5]. Then Eq. (59) becomes:

$$\begin{aligned} \lim_{T_s \to 0} \delta \mathbf{x}(s) &= \{ s\mathbf{I} - (D'\mathbf{A}_0 + D\mathbf{A}_1) \}^{-1} \\ &\quad \cdot \{ (\mathbf{A}_1 - \mathbf{A}_0)\, \mathbf{X} + (\mathbf{B}_1 - \mathbf{B}_0)\, \mathbf{u} \}\, \hat{d}(s) \end{aligned} \tag{60}$$

which is exactly the prediction given by the *State Space Averaging Modelling Method.* Therefore, the prediction of the *State Space Averaging Modelling Method* is exact when the switching frequency of the converter system approaches infinity.

Consider the circuit shown in Fig. 8 as an example:

$$\begin{array}{llll} \mathbf{A}_0 = -\frac{R+R'}{L} & & \mathbf{A}_1 = -\frac{R}{L} \\ \mathbf{B}_0 = 0 & & \mathbf{B}_1 = \frac{1}{L} \\ \mathbf{x} = i & & \mathbf{u} = V_g \\ D_0 = \frac{T_0}{T_s} & & D_1 = \frac{T_1}{T_s} \\ m_0^t = \frac{V_m}{T_s} & & R' = 0\Omega \end{array}$$

The steady state $\mathbf{X}_0$ is given by:

$$\begin{aligned} \mathbf{X}_0 &= \left[\mathbf{I} - e^{\mathbf{A}_1 T_1} e^{\mathbf{A}_0 T_0}\right]^{-1} \\ &\quad \cdot \left\{\mathbf{A}_1^{-1}\left[e^{\mathbf{A}_1 T_1} - \mathbf{I}\right]\mathbf{B}_1\,\mathbf{u} \right. \\ &\quad \left. + e^{\mathbf{A}_1 T_1}\mathbf{A}_0^{-1}\left[e^{\mathbf{A}_0 T_0} - \mathbf{I}\right]\mathbf{B}_0\,\mathbf{u}\right\} \end{aligned} \quad (61)$$

The steady state $\mathbf{X}_1$ is given by:

$$\mathbf{X}_1 = e^{\mathbf{A}_0 T_0}\mathbf{X}_0 + \mathbf{A}_0^{-1}\left[e^{\mathbf{A}_0 T_0} - \mathbf{I}\right]\mathbf{B}_0\mathbf{u} \quad (62)$$

Therefore, the steady state I_0 is:

$$I_0 = \left[1 - e^{-\frac{RT_1 + (R+R')T_0}{L}}\right]^{-1}\left[1 - e^{\frac{RT_1}{L}}\right]\frac{V_g}{R} \quad (63)$$

Then, according to Eq. (58), the pulse transfer function is:

$$G(s) = \tilde{H}(s)\,(1 - e^{-sT_s}\tilde{\Phi})^{-1}\,\tilde{k} \quad (64)$$

where:

$$\begin{aligned} \tilde{H}(s) &= \left\{\frac{1 - e^{-(s+\frac{R+R'}{L})T_0}}{s + \frac{R+R'}{L}} + \frac{1 - e^{-(s+\frac{R}{L})T_1}}{s + \frac{R}{L}}\, e^{-(s+\frac{R+R'}{L})T_0}\right\} \\ \tilde{\Phi} &= e^{\frac{RT_1 + (R+R')T_0}{L}} \\ \tilde{k} &= \frac{T_s V_g}{L V_m} \\ &\quad \cdot \left\{1 + \frac{R'}{R}\left[1 - e^{-\frac{RT_1 + (R+R')T_0}{L}}\right]^{-1}\left[1 - e^{\frac{RT_1}{L}}\right]\right\} \end{aligned}$$

The resistance $R' = 0\Omega$ in this example, and the pulse transfer function from $\delta r_0^*(s) = \delta v_{ref}^*(s)$ to $\delta v_o(s)$, according to Eq. (64) is:

$$R\,G(s) = \frac{T_s\,R/L}{s + R/L}\,\frac{V_g}{V_m} \quad (65)$$

where V_m is the peak-to-peak voltage of the PWM ramp. The Bode plots up to three times the switching frequency of the theoretical *"transfer function"* from v_{ref} to v_o, i.e. $RG(s)/T_s$, and the measurement are shown in Fig. 9. They agree well with each other. The extra phase in the measurement plot at high frequencies comes from the propagation delay in the experimental setup.

3.4 Constant Frequency Programmed Converters

The control strategy for constant switching frequency programmed converters may be described by $M_{2i} = M^c$ and $M_{2i+1} = M^u$. As discussed in Section 2.1, it is possible for this converter to have multiple stable steady state solutions for a given operating condition. In this section, only one of the solutions, the two-switched-state solution, will be treated. In this case, $T_s = T_1 + T_2 = T_c$.

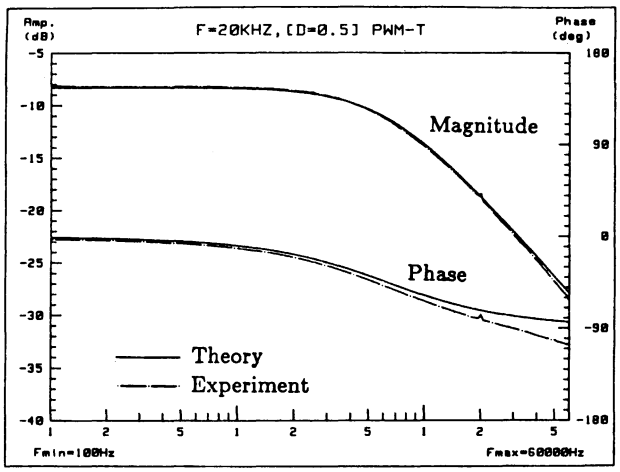

Fig. 9: The Bode plot of the theoretical prediction and the experimental results of the converter shown in Fig. 8 operating at $D = T_1/T_s = .5$.

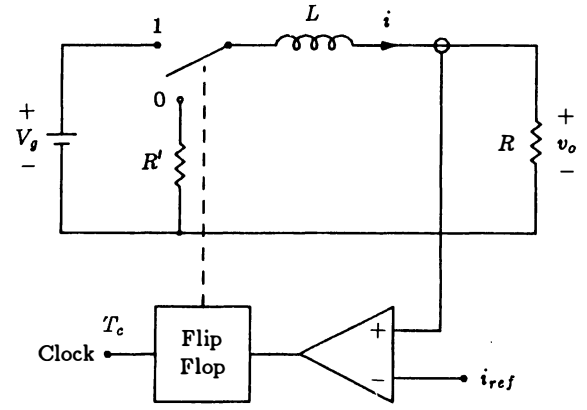

Fig. 10: A constant switching frequency programmed R-L converter: V_g = 15Volts, L = 1.41mH, R = 54Ω, R' = 51.4Ω, $T_s = T_c$ = 20kHz.

According to Eq. (57), the frequency response of the converter system with control-input r_0 is:

$$\begin{aligned} \delta\mathbf{x}(s) &= \left\{\tilde{\mathbf{H}}_0(s) + e^{sT_0}\,\tilde{\mathbf{H}}_1(s)\,e^{\mathbf{A}_0 T_0}\right\} \\ &\quad \cdot \left\{\mathbf{I} - e^{-sT_s}\,\tilde{\mathbf{\Phi}}\right\}^{-1}\,\tilde{\mathbf{k}}\,\delta r_0^*(s) \end{aligned} \quad (66)$$

where

$$\begin{aligned} \tilde{\mathbf{H}}_i(s) &= [s\mathbf{I} - \mathbf{A}_i]^{-1}\left[\mathbf{I} - e^{-sT_i}\,e^{\mathbf{A}_i T_i}\right] \\ \tilde{\mathbf{\Phi}} &= \tilde{\mathbf{K}}_0^c\,e^{\mathbf{A}_1 T_1}\,e^{\mathbf{A}_0 T_0} \\ \tilde{\mathbf{k}} &= \tilde{\mathbf{k}}_0^c \end{aligned}$$

where $\tilde{\mathbf{K}}_0^c$ and $\tilde{\mathbf{k}}_0^c$ are as defined in in Eq. (43) and Eq. (44) respectively. The steady state $\mathbf{X}_0$ that is used in calculating $\tilde{\mathbf{K}}_0^c$ and $\tilde{\mathbf{k}}_0^c$ may be find by using Eq. (61) if $\mathbf{A}_0$ and $\mathbf{A}_1$ is invertible.

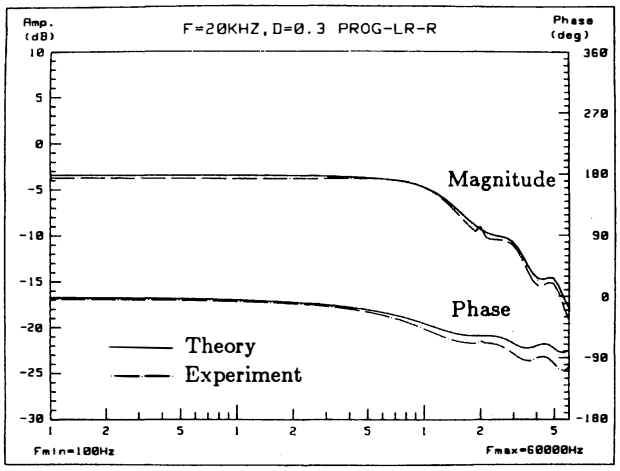

Fig. 11: The Bode plot of the theoretical prediction and the experimental results of the converter shown in Fig. 10 operating at $D = T_1/T_s = .3$.

As an example, consider the circuit shown in Fig. 10.

$$\begin{array}{llll} \mathbf{A}_0 = -\frac{R+R'}{L} & & \mathbf{A}_1 = -\frac{R}{L} \\ \mathbf{B}_0 = 0 & & \mathbf{B}_1 = \frac{1}{L} \\ \mathbf{x} = i & & \mathbf{u} = V_g \\ D_0 = \frac{T_0}{T_s} & & D_1 = \frac{T_1}{T_s} \\ m_0^c = 0 & & \mathbf{f}_0 = 1 \end{array}$$

Using Eq. (61), the steady state I_0 is:

$$I_0 = \left[1 - e^{-\frac{RT_1+(R+R')T_0}{L}}\right]^{-1} \left[1 - e^{\frac{RT_1}{L}}\right] \frac{V_g}{R} \qquad (67)$$

According to Eq. (66), the pulse transfer function is:

$$G(s) = \tilde{H}(s)\,(1 - e^{-sT_s}\tilde{\Phi})^{-1}\,\tilde{k} \qquad (68)$$

where:

$$\begin{aligned} \tilde{H}(s) &= \left\{ \frac{1 - e^{-(s+\frac{R+R'}{L})T_0}}{s + \frac{R+R'}{L}} + \frac{1 - e^{-(s+\frac{R}{L})T_1}}{s + \frac{R}{L}}\, e^{-(s+\frac{R+R'}{L})T_0} \right\} \\ \tilde{\Phi} &= e^{\frac{RT_1+(R+R')T_0}{L}}\,(1 - \bar{k}_0\, p_0) \\ \tilde{k} &= m_0\,\bar{k}_0 \\ \bar{k}_0 &= \frac{R'}{L}\,I_0 + \frac{1}{L}\,V_g \\ m_0 &= \left(-\frac{R}{L}\,I_0 + \frac{1}{L}\,V_g\right)^{-1} \\ p_0 &= \left(-\frac{R}{L}\,I_0 + \frac{1}{L}\,V_g\right)^{-1} \end{aligned}$$

Shown in Fig. 11 is the Bode plot of the theoretical *"transfer function"* $\frac{1}{T_s}\,G(s)$ and the corresponding measurement up to three times the switching frequency. The difference between the two plots in phase at high frequencies is a result of propagation delay in the circuit. For this example, all the three modelling methods which are discussed in the introduction, namely, *State Space Averaging Model*[1,4,5], *Sampled-Data Modelling*[2], and *Small Signal Analysis of Resonant Converters*[3] fail. It is well known that the *State Space Averaging Model* does not work for programmed converters when

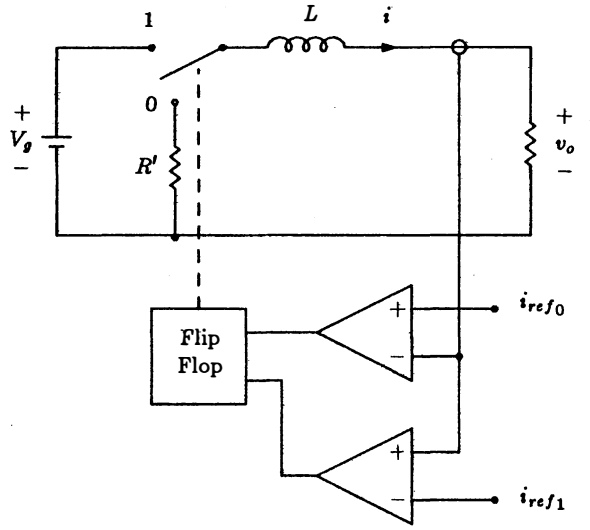

Fig. 12: A bang-bang controlled R-L converter: $V_g = 15$Volts, $L = 1.43$mH, $R = 56\Omega$, $R' = 6.7\Omega$, $T_s = 25$kHz.

the frequency of the signal injected for measurement is close to and higher than half the switching frequency[2]. *Sampled-Data Modelling* fails because the time constants in the converter circuit are much shorter than the switching period — this converter does not satisfy the small ripple assumption. *Small Signal Analysis of Resonant Converter* can handle the large ripple in the circuit but its prediction of the phase of any converter system is always a multiple of 180 degrees for the injected signal at a multiple of half the switching frequency. It is obvious that this is clearly not the case from the Bode plots in Fig. 11.

3.5 Bang-Bang Controlled Converters

The control strategy of a bang-bang controlled two-switched-state converter system may be characterized by $M_i = M^c$, $N_s = 2$. The first step to find the frequency response of the system is to find $\tilde{\mathbf{K}}_0^c$, $\tilde{\mathbf{K}}_1^c$, $\tilde{\mathbf{k}}_0^c$, and $\tilde{\mathbf{k}}_1^c$. These quantities are defined in Eq. (43) and Eq. (44). The $\mathbf{X}_0$ and $\mathbf{X}_1$ used in calculating these quantities may be found by using Eq. (61) and Eq. (62) provided $\mathbf{A}_0$ and $\mathbf{A}_1$ are invertible. The frequency response of $\delta\mathbf{x}$ with respect to δr_0, according to Eq. (57) is:

$$\begin{aligned} \delta\mathbf{x}(s) &= \left\{\tilde{\mathbf{H}}_0(s) + e^{-sT_0}\,\tilde{\mathbf{H}}_1(s)\,\tilde{\mathbf{K}}_1^c\, e^{\mathbf{A}_0 T_0}\right\} \\ &\quad \cdot \left\{\mathbf{I} - e^{-sT_s}\,\tilde{\mathbf{K}}_0^c\, e^{\mathbf{A}_1 T_1}\,\tilde{\mathbf{K}}_1^c\, e^{\mathbf{A}_0 T_0}\right\}^{-1} \tilde{\mathbf{k}}_0^c\,\delta r_0^*(s) \qquad (69) \end{aligned}$$

where $\tilde{\mathbf{H}}_i(s) = [s\mathbf{I} - \mathbf{A}_i]^{-1}\{\mathbf{I} - e^{-sT_i}\, e^{\mathbf{A}_i T_i}\}$. The frequency response of $\delta\mathbf{x}$ with respect to r_1 may be obtained by interchanging the subscripts 0 and 1 in Eq. (69):

$$\begin{aligned} \delta\mathbf{x}(s) &= \left\{\tilde{\mathbf{H}}_1(s) + e^{-sT_0}\,\tilde{\mathbf{H}}_0(s)\,\tilde{\mathbf{K}}_0^c\, e^{\mathbf{A}_1 T_1}\right\} \\ &\quad \cdot \left\{\mathbf{I} - e^{-sT_s}\,\tilde{\mathbf{K}}_1^c\, e^{\mathbf{A}_0 T_0}\,\tilde{\mathbf{K}}_0^c\, e^{\mathbf{A}_1 T_1}\right\}^{-1} \tilde{\mathbf{k}}_1^c\,\delta r_1^*(s) \qquad (70) \end{aligned}$$

Figure 12 is the circuit of a bang-bang controlled converter,

in which:

$$\begin{array}{llll} \mathbf{A}_0 = -\frac{R+R'}{L} & & \mathbf{A}_1 = -\frac{R}{L} \\ \mathbf{B}_0 = 0 & & \mathbf{B}_1 = \frac{1}{L} \\ \mathbf{x} = i & & \mathbf{u} = V_g \\ m_0^c = 0 & & m_1^c = 0 \\ \mathbf{f}_0 = 1 & & \mathbf{f}_1 = 1 \end{array}$$

Using Eq. (61) and Eq. (62), the steady state I_0 and I_1 are:

$$I_0 = \left[1 - e^{-\frac{R}{L}T_1} e^{-\frac{R+R'}{L}T_0}\right]^{-1} \left[1 - e^{-\frac{R}{L}T_1}\right] \frac{V_g}{R} \quad (71)$$

$$I_1 = e^{-\frac{R+R'}{L}T_0} I_0 \quad (72)$$

Then:

$$\tilde{\mathbf{K}}_0^c = -\frac{I_0(R+R')}{V_g - I_0 R} \quad (73)$$

$$\tilde{\mathbf{K}}_1^c = -\frac{V_g - I_1 R}{I_1(R+R')} \quad (74)$$

$$\tilde{\mathbf{k}}_0^c = \frac{V_g + I_0 R'}{V_g - I_0 R} \quad (75)$$

$$\tilde{\mathbf{k}}_1^c = \frac{V_g + I_1 R'}{I_1(R+R')} \quad (76)$$

According to Eq. (69), the frequency response of δi with respect to δi_{ref_0} is:

$$\delta \mathbf{x}(s) = G_0(s)\, \delta i_{ref_0}^*(s) \quad (77)$$

where

$$G_0(s) = \frac{V_g + I_0 R'}{V_g - I_0 R} \cdot \left\{\tilde{H}_0(s) - e^{-(s+\frac{R+R'}{L})T_0} \frac{V_g - I_1 R}{I_1(R+R')} \tilde{H}_1(s)\right\} \cdot \left\{1 - e^{-sT_s} e^{-\frac{R}{L}T_1} e^{-\frac{R+R'}{L}T_0} \frac{I_0}{I_1} \frac{V_g - I_1 R}{V_r - I_0 R}\right\}^{-1}$$

$$\tilde{H}_0(s) = \frac{1 - e^{-(s+\frac{R+R'}{L})T_0}}{s + \frac{R+R'}{L}}$$

$$\tilde{H}_1(s) = \frac{1 - e^{-(s+\frac{R}{L})T_1}}{s + \frac{R}{L}}$$

The Bode plots of the theoretical *"transfer function"* $G_0(s)/T_s$ and the experimental measurement, up to at least two times the switching frequency, are shown in Fig. 13 and Fig. 14.

An interesting feature in the Bode plots is that the phase of the response is increasing, up to the switching frequency, for the case $D = T_1/T_s > .5$ and decreasing for the case of $D < .5$. The time constants in the converter circuit are smaller than the switching period. The theoretical predictions and experimental results agree with each other.

The frequency response of δi with respect to δi_{ref_1}, according to Eq. (69), is:

$$\delta \mathbf{x}(s) = G_1(s)\, \delta i_{ref_1}^*(s) \quad (78)$$

where

$$G_1(s) = \frac{V_g - I_1 R}{I_1(R+R')} \cdot \left\{\tilde{H}_1(s) - e^{-(s+\frac{R}{L})T_1} \frac{I_0(R+R')}{V_g - I_0 R} \tilde{H}_0(s)\right\} \cdot \left\{1 - e^{-sT_s} e^{-\frac{R}{L}T_1} e^{-\frac{R+R'}{L}T_0} \frac{I_0}{I_1} \frac{V_g - I_1 R}{V_r - I_0 R}\right\}^{-1}$$

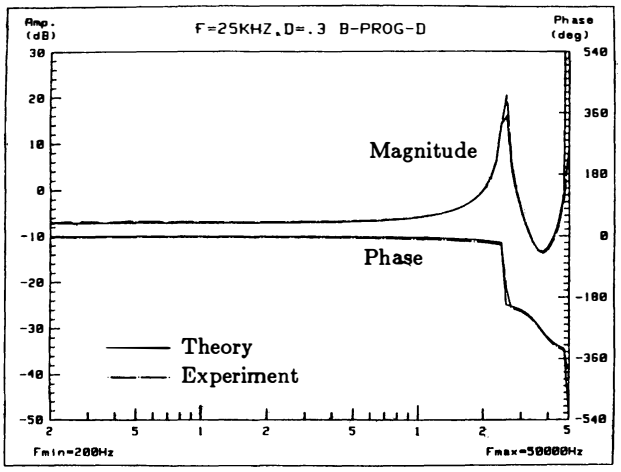

Fig. 13: The Bode plots of the theoretical prediction and the experimental results of the converter shown in Fig. 12 operating at $D = T_1/T_s = .3$; only i_{ref_0} is modulated.

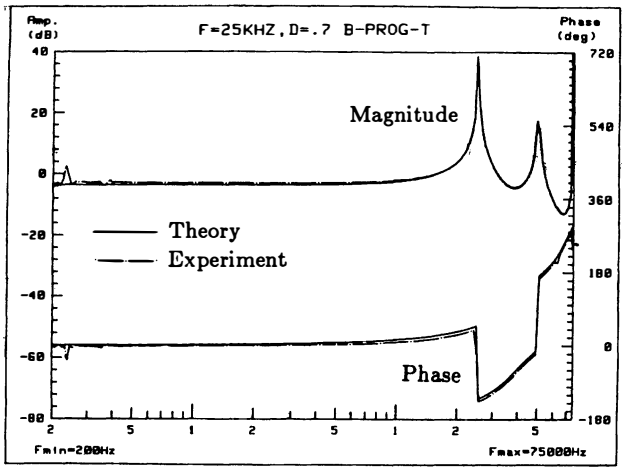

Fig. 14: The Bode plots of the theoretical prediction and the experimental results of the converter shown in Fig. 12 operating at $D = T_1/T_s = .7$; only i_{ref_0} is modulated.

If both δi_{ref_0} and δi_{ref_1} are modulated with the same signal δi_{ref}, then the *"transfer function"* from δi_{ref} to δi is $G/T_s = [G_0(s) + G_1(s)]/T_s$. The Bode plots of theoretical prediction and experimental measurement of this *"transfer function"*, up to three times the switching frequency are shown Fig. 15. The theoretical prediction and experimental results are almost indistinguishable in the figure.

All the three modelling methods discussed before, namely, *State Space Averaging Modelling Method* [1,4,5], *Sampled-Data Modelling of Switching Regulators*[2] and *Small-Signal Analysis of Resonant Converters*[3] fail to predict the frequency response of this bang-bang controlled converter.

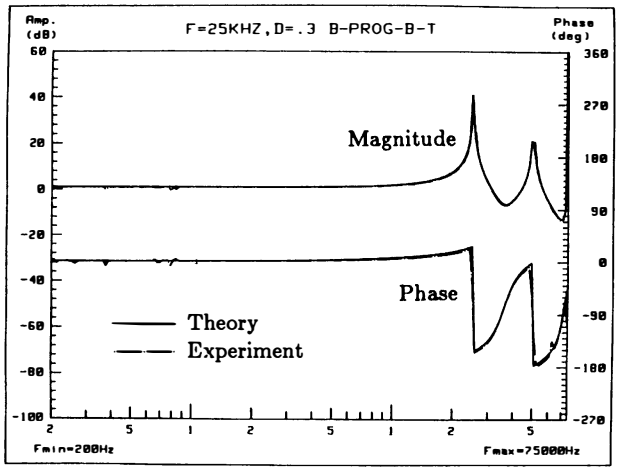

Fig. 15: The Bode plots of the theoretical prediction and the experimental results of the converter shown in Fig. 12 operating at $D = T_1/T_s = .3$; both i_{ref_0} and i_{ref_1} are modulated with the same signal.

4 General Two-Switched-State Converters

In Section 3, a systematic procedure for constructing the difference equation that describes the small-signal motion of the system about its steady state solution is developed. However, the formulation in Section 3 cannot treat the modified-time modulation and cannot take into account the output equation if the output signal is discontinuous. In this section, the formulation in Section 3 is modified to overcome these problems. First, the difference equation is Section 3 is augmented. In Section 4.1, a systematic procedure for constructing this augmented difference equation is presented. Second, the *equivalent hold* is generalized to take into account of discontinuities in the output signal. This *generalized equivalent hold* is discussed in Section 4.2. Since the basic concept is already introduced in Section 3, there is no attempt to derive the results in detail in this section. Instead, the results are present in an algorithmic way.

4.1 Small-Signal Motion

All the four modulation methods described in Section 1.2 may be described by Eq. (79) and Eq. (80) below:

$$\delta t_i[n] = m_i\,\delta r_i[n] + h_i\,\delta t_{i-1}[n] - \mathbf{p}_i^T\,\delta\tilde{\mathbf{x}}_{i-1}[n] \quad (79)$$

$$\delta\mathbf{x}_i[n] = \delta\tilde{\mathbf{x}}_{i-1}[n] + \bar{\mathbf{k}}_i\,\delta t_i[n] \quad (80)$$

1. For the unmodulated case, i.e. $M_i = M^u$:

$$\begin{aligned} m_i &= 0 \\ h_i &= 0 \\ \mathbf{p}_i &= \mathbf{0} \end{aligned}$$

2. For the time-modulated case, i.e. $M_i = M^t$:

$$\begin{aligned} m_i &= (m_i^t)^{-1} \\ h_i &= 0 \\ \mathbf{p}_i &= \mathbf{0} \end{aligned}$$

3. For the constraint-modulated case, i.e. $M_i = M^c$:

$$\begin{aligned} m_i &= \left(m_i^c + \mathbf{f}_i^T\left[\mathbf{A}_{i-1}\mathbf{X}_i + \mathbf{B}_{i-1}\mathbf{u}\right]\right)^{-1} \\ h_i &= 0 \\ \mathbf{p}_i &= m_i\,\mathbf{f}_i^T \end{aligned}$$

4. For modified-time-modulated case, i.e. $M_i = M^m$:

$$\begin{aligned} m_i &= (m_i^m)^{-1} \\ h_i &= h_i \\ \mathbf{p}_i &= \mathbf{0} \end{aligned}$$

In this framework, it is obvious that a closed-loop PWM converter system is the same as a programmed converter system with an added stabilizing ramp. However, an open-loop PWM converter system is very different from its closed-loop version. As a result, the steday state solution of both closed-loop PWM converter systems and programmed converter systems may go unstable under certain conditions while open-loop PWM converter systems are always stable.

For those converter systems that use modified-time-modulation to control the transition from one switched-state to the other, a difference equation involving only $\delta\mathbf{x}_i[n]$ and $\delta r_i[n]$ is not sufficient to describe the small-signal motion of the system. There is a relationship between $\delta t_i[n]$ and $\delta t_{i-1}[n]$. The difference equation has to be augmented to overcome this problem. The first step in augmenting the difference equation is to augment the states of the equation from $\delta\mathbf{x}_i[n]$ to $\delta\mathbf{x}_i^*[n]$, where:

$$\delta\mathbf{x}_i^*[n] \equiv \begin{bmatrix} \delta\mathbf{x}_i[n] \\ \delta t_i[n] \end{bmatrix} \quad (81)$$

By using Eq. (79) and Eq. (80), then:

$$\begin{aligned} &\delta\mathbf{x}_i^*[n] \\ &= \begin{bmatrix} \delta\mathbf{x}_i[n] \\ \delta t_i[n] \end{bmatrix} \\ &= \begin{bmatrix} \delta\tilde{\mathbf{x}}_{i-1}[n] + \bar{\mathbf{k}}_i\left\{m_i\,\delta r_i[n] + h_i\,\delta t_{i-1}[n] - \mathbf{p}_i^T\,\delta\tilde{\mathbf{x}}_{i-1}[n]\right\} \\ m_i\,\delta r_i[n] + h_i\,\delta t_{i-1}[n] - \mathbf{p}_i^T\,\delta\tilde{\mathbf{x}}_{i-1}[n] \end{bmatrix} \\ &= \begin{bmatrix} \mathbf{I} - \bar{\mathbf{k}}_i\,\mathbf{p}_i^T & h_i\,\bar{\mathbf{k}}_i \\ -\mathbf{p}_i^T & h_i \end{bmatrix} \begin{bmatrix} \delta\tilde{\mathbf{x}}_{i-1}[n] \\ \delta t_{i-1}[n] \end{bmatrix} + \begin{bmatrix} m_i\,\bar{\mathbf{k}}_i \\ m_i \end{bmatrix} \delta r_i[n] \\ &= \begin{bmatrix} \{\mathbf{I} - \bar{\mathbf{k}}_i\,\mathbf{p}_i^T\}\,e^{\mathbf{A}_{i-1}T_{i-1}} & h_i\,\bar{\mathbf{k}}_i \\ -\mathbf{p}_i^T\,e^{\mathbf{A}_{i-1}T_{i-1}} & h_i \end{bmatrix} \delta\mathbf{x}_{i-1}^*[n] \\ &\qquad + \begin{bmatrix} m_i\,\bar{\mathbf{k}}_i \\ m_i \end{bmatrix} \delta r_i[n] \end{aligned} \quad (82)$$

For convenience, define:

$$\mathbf{\Phi}_{i-1} = \begin{bmatrix} \{\mathbf{I} - \bar{\mathbf{k}}_i \mathbf{p}_i^T\} e^{\mathbf{A}_{i-1}T_{i-1}} & h_i \bar{\mathbf{k}}_i \\ -\mathbf{p}_i^T e^{\mathbf{A}_{i-1}T_{i-1}} & h_i \end{bmatrix} \quad (83)$$

$$\mathbf{k}_i = \begin{bmatrix} m_i \bar{\mathbf{k}}_i \\ m_i \end{bmatrix} \quad (84)$$

Then Eq. (82) may be rewritten as:

$$\delta \mathbf{x}_i^*[n] = \mathbf{\Phi}_{i-1}\, \delta \mathbf{x}_{i-1}^*[n] + \mathbf{k}_i\, \delta r_i[n] \quad (85)$$

Consider the case in which only M_{2j}'s are modulated (the case in which M_{2j+1}'s are modulated may be taken into account later by superposition); then, the equation that describes the small-signal motion of the system is:

$$\delta \mathbf{x}_0^*[n] = \mathbf{\Phi}\, \delta \mathbf{x}_0^*[n-1] + \mathbf{k}\, \delta r_0[n] \quad (86)$$

where

$$\mathbf{\Phi} = \mathbf{\Phi}_1 \mathbf{\Phi}_0$$
$$\mathbf{k} = \mathbf{k}_0$$

4.2 The Frequency Response

If the output matrix $\mathbf{C}(t)$ and/or transmission matrix $\mathbf{D}(t)$ in Eq. (1) are discontinuous, then, the output $\mathbf{y}(t)$ is discontinuous; however, the state $\mathbf{x}$ is always continuous. The *equivalent hold* introduced in Section 3 works only for continuous output. Therefore, it is necessary to generalize the *equivalent hold* to take into account the discontinuity.

In the *small-signal limit* the effect of the discontinuity on $\delta\mathbf{y}$ is the addition of a pulse train of *"width"* $|\,\delta t_i\,|$ and *"height"* $\mathrm{sgn}(\delta t_i)\,\{(\mathbf{C}_{i-1}-\mathbf{C}_i)\mathbf{X}_i + (\mathbf{D}_{i-1}-\mathbf{D}_i)\mathbf{u}\}$. It can be shown that the effect of this pulse train on $\delta\mathbf{y}(s)$ is the same as a train of δ-functions of magnitude $\delta t_i\,\{(\mathbf{C}_{i-1}-\mathbf{C}_i)\mathbf{X}_i + (\mathbf{D}_{i-1}-\mathbf{D}_i)\mathbf{u}\}$. Therefore, $\delta\mathbf{y}'(s)$, the effect of $\delta\mathbf{x}_i[n]$ and $\delta t_i[n]$ on the output signal $\mathbf{y}$, is:

$$\delta\mathbf{y}'(s) = e^{-s\mathbf{T}_{i+nN_s}} \Big\{ \mathbf{C}_i\,[s\mathbf{I}-\mathbf{A}_i]^{-1}\,[\mathbf{I} - e^{sT_i}\,e^{\mathbf{A}_i T_i}]\,\delta x_i[n] + [(\mathbf{C}_{i-1}-\mathbf{C}_i)\mathbf{X}_i + (\mathbf{D}_{i-1}-\mathbf{D}_i)\mathbf{u}]\,\delta t_i[n]\} \quad (87)$$

The difference equation, introduced in Section 3.1, that describes the small-signal motion of the system is not sufficient for finding $\delta\mathbf{y}$ because it does not carry the information about $\delta t_i[n]$. It is necessary to use the augmented difference equation developed in Section 4.1 with the augmented state $\delta\mathbf{x}_i^*[n]$ to find $\delta\mathbf{y}$. In this case, Eq. (87) may be rewritten as:

$$\delta\mathbf{y}'(s) = e^{-s\mathbf{T}_{i+nN_s}}\,\mathbf{H}_i(s)\,\delta\mathbf{x}_i^*[n] \quad (88)$$

where

$$\mathbf{H}_i(s) = \left[\; \mathbf{C}_i\,\tilde{\mathbf{H}}_i(s),\;\; (\mathbf{C}_{i-1}-\mathbf{C}_i)\mathbf{X}_i + (\mathbf{D}_{i-1}-\mathbf{D}_i)\mathbf{u} \;\right]$$
$$\tilde{\mathbf{H}}_i(s) = [s\mathbf{I}-\mathbf{A}_i]^{-1}\,[\mathbf{I} - e^{sT_i}\,e^{\mathbf{A}_i T_i}]$$

Therefore, the control-input-to-output frequency response of an ideal two-switched-state dc-to-dc converter system corresponding to a steady state solution is:

$$\delta\mathbf{y}(s) = \Big\{\mathbf{H}_0(s) + e^{-sT_0}\,\mathbf{H}_1(s)\,\mathbf{\Phi}_0\Big\}\,\Big\{I - e^{-sT_s}\,\mathbf{\Phi}\Big\}^{-1}\,\delta r_0^*(s) \quad (89)$$

where

$$\mathbf{\Phi} = \mathbf{\Phi}_1\mathbf{\Phi}_0$$
$$\delta r_0^* = \frac{1}{T_s}\sum_{n=-\infty}^{\infty} \delta r_0(s + \frac{2n\pi}{T_s})$$

5 Conclusions

In this paper, the *Small-Signal Frequency Response Theory*, a mathematical theory for linearization of ideal dc-to-dc converter systems in the frequency domain is introduced. This theory overcomes the problems encountered when other modelling methods are employed, namely, *State Space Averaging Modelling Method, Sampled-Data Modelling of Switching Regulator*, and *Small-Signal Analysis of Resonant Converters*. The theory assumes that the steady state solution to the ideal dc-to-dc converter system is known. Given the steady state solution, the theory will give the control-input-to-output frequency response. The result given by the theory resembles the frequency response of a sampled-data system with a very complicated hold.

The steps to find the frequency response for any ideal dc-to-dc converter are laid out in an algorithmic way in Section 4. The first step is to find the difference equation that describes the small-signal motion of the system about its steady state solution. In Section 3, the difference equations in analytic form for some representative popular converter systems are presented. In Section 4.1, a systematic procedure to construct the difference equation for any ideal dc-to-dc converter system (as defined in Section 1) is presented. The second step is to find the *equivalent hold* that relates the difference equation and the output signal. In Section 3, the *equivalent hold* is derived without considering the output equation. This *equivalent hold* works for converters with continuous output signals. However, it cannot take into account possible discontinuity of the output signal. In Section 4, the *generalized equivalent hold* is introduced to be used with the augmented difference equation described in Section 4.1 to overcome this problem.

In introducing the *Small-Signal Frequency Response Theory* through a simple example in Section 2, it is found that that the operating point cannot fully specify the steady state solution of a dc-to-dc converter system. What one usually refers to as the instability of a dc-to-dc converter system at a certain operating point is actually the instability of a particular solution corresponding to that operating point and the other stable solutions corresponding to the same operating point are unacceptable.

In developing a general algorithm for writing down the difference equation that describes the small-signal motion of a converter system, it was found that there is no difference between the mathematical description for PWM converters in closed loop operation and programmed converters. This fact is consistent with experimental observations that in a programmed converter, if the slope of the added stabilization ramp is varied, its frequency response will vary from that of a typical current programmed converter to that of a typical closed loop PWM converter. In both *State Space Averaging Modelling Method*[4,5], and *Sampled-Data Modelling of Switching Converter*[2], a special model of the modulator is needed for modelling a programmed converter with an added stabilization ramp.

From the formulation of *Small-Signal Frequency Response Theory* laid out in Section 4, it is obvious that it is a powerful tool that has may applications. The theory can be extended to multiple switched-state, multiple switched-network converters. In fact, when the theory was developed, it was developed for multiple switched-state converter systems. Because the theory

does not differentiate between PWM converters and resonant converters in its formulation, the theory can be used to analyze PWM converter systems with snubbers — a hybrid of PWM and resonant converters. Since *Small-Signal Frequency Response Theory* can exactly linearize ideal dc-to-dc converters in the frequency domain, it is now possible to study whether a certain ideal circuit model is advisable for a certain physical converter circuit.

References

[1] R. D. Middlebrook and Slobodan Ćuk, "A General Unified Approach to Modelling Switching-Converter Power Stages," IEEE Power Electronics Specialists Conference, 1976 Record, pp. 18-34 (IEEE Publication 76CH1084-3 AES); also International Journal of Electronics, Vol. 42, No. 6, pp. 521-550, June 1977.

[2] Arthur R. Brown and R. D. Middlebrook, "Sampled-Data Modeling of Switching Converters," IEEE Power Electronics Specialists Conference, 1981 Record, pp. 349-369 (IEEE Publication 81CH1652-7).

[3] Vatché Vorpérian and Slobodan Ćuk, "Small-Signal Analysis of the Series Resonant Converter," IEEE Power Electronics Specialists Conference, 1983 Record, pp. 269-282 (IEEE Publication 83CH1877-0).

[4] Shi-Ping Hsu, Arthur Brown, Loman Rensink, and R. D. Middlebrook, "Modelling and Analysis of Switching Dc-to-Dc Converters in Constant- Frequency Current-Programmed Mode," IEEE Power Electronics Specialists Conference, 1979 Record, pp. 284-301 (IEEE Publication 79CH1461-3 AES).

[5] R. D. Middlebrook, "Topics in Multi-Loop Regulators and Current-Mode Programming," IEEE Power Electronics Specialists Conference, 1985 Record, pp. 716-732 (IEEE Publication 85CH2117-0).

[6] C. E. Shannon, "A Mathematical Theory of Communication," The Bell System Technical Journal, No. 3, Vol. 27, pp. 379-433, July 1948. Also The Bell System Technical Journal, No. 4, Vol. 27, pp. 623-656, October 1948.

[7] Gene F. Franklin and J. David Powell, *Digital Control of Dynamic Systems,* Addison-Wesley, Reading, MA, 1981.